sciendo

Transport and Telecommunication, 2023, volume 24, no. 3, 297–308
Transport and Telecommunication Institute, Lomonosova 1, Riga, LV-1019, Latvia
DOI 10.2478/ttj-2023-0024

DESIGN, MODELLING AND RESEARCH OF AN ANTENNA SYSTEM FOR TRANSMITTING AND RECEIVING INFORMATION IN SATELLITE SYSTEMS

Islam Islamov[1], Arzu Safarli[2]

[1]Department of Radio Engineering and Telecommunication, Azerbaijan Technical University
AZ1073, H. Javid ave. 25, Baku, Azerbaijan
icislamov@mail.ru
[2]Department of Research and Development, Azerbaijan Technical University
AZ1073, H. Javid ave. 25, Baku, Azerbaijan
arzusafarli@aztu.edu.az

The work deals with the design, modelling and research of an antenna system for transmitting and receiving information in satellite systems. It was revealed that this antenna array with a transmitter of 85 *dBWt* is guaranteed to solve the target problem of providing mobile satellite communications with both one global beam and a plurality of beams with a width of 0,7 × 0,7°. It should be added that the advantage of forming multiple beams compared to a global beam with a single phased antenna array is: higher data rate, relatively low requirements for antenna systems of ground stations, greater noise immunity of the radio link, the ability to dynamically control the signal power in each beam.

Keywords: Antenna system, modelling, satellite connection, phase shifter, transmitter

1. Introduction

In an active phased array antenna (APAA), each element or group of elements has its own miniature microwave transmitter, eliminating the need for a single large transmitter tube used in passive phased array radars. Each APAA element consists of a module that contains an antenna slot, a phase shifter, a transmitter, and often also a receiver (Mohammad, 2020; Pinuela *et al.*, 2013; Zhou *et al.*, 2016; Yi-Ming *et al.*, 2020; Zhao *et al.*, 2020; Ao *et al.*, 2020).

In essence, APAA is a radio engineering system in which a radio transmitter and a high-frequency receiver are integrated into an antenna array in the form of a distributed structure, which includes transceiver active modules as main nodes (Botao *et al.*, 2020; Muhammad *et al.*, 2021; Yuchen *et al.*, 2020).

In this regard, the development of APAA requires an integrated approach that takes into account the mutual conjugation of the electrodynamics properties of the emitters of the antenna fabric and the radio characteristics of the transceiver antenna modules for various types of signals, edge effects, technological and temporal destabilizing factors of module failures.

A significant improvement in the quality, reliability, stability, and efficiency of radio communications, an increase in its range and volume of transmitted information are primarily associated with the development of satellite communication systems in recent decades. In mobile and space radio complexes, APAA are increasingly being used, which make it possible to implement a multifunctional mode of operation and meet the increasing requirements for the necessary energy and weight and size characteristics of communication equipment (Avishek *et al.*, 2021; Kai *et al.*, 2021; Daniel *et al.*, 2022; Islamov *et al.*, 2019; Islamov *et al.*, 2020).

Since the energy resources of mobile points are, as a rule, limited, maintaining a high APAA potential in the scanning sector is associated with minimizing all losses both in the transmission path and in the radio link section. This gives rise to the following basic requirements for APAA:

- the maximum value of the coefficient of ellipticity of the radiation field and the minimization of its change in the scanning sector;
- minimum losses due to mismatch of emitters during scanning;

- stable mode of operation of APAA antenna modules under load changes caused by the interaction of emitters and edge effects.

The fulfillment of the listed requirements is possible only by optimizing the parameters of the APAA, taking into account all the factors affecting its operation (Khalilov *et al.*, 2020; Islamov *et al.*, 2018; Ismibayli *et al.*, 2018; Islamov *et al.*, 2018; Islamov *et al.*, 2019).

The development of space technology predetermined the widespread use of artificial Earth satellites in geostationary orbit or highly elliptical orbits as repeaters in communication lines (Abdulrahman *et al.*, 2021; Islamov *et al.*, 2021; Zulfugarli *et al.*, 2021; Hunbataliyev *et al.*, 2021).

A number of specific requirements are imposed on antenna systems (including APAA) of communication spacecraft:

- ensuring a high antenna gain due to the large remoteness of the spacecraft from subscriber stations on the earth's surface (for a geostationary orbit, the distance is about 35800 *km*, for highly elliptical orbits up to 40000 *km* at apogee), which leads to large losses along the propagation path (attenuation of the useful signal, depending on the radiation frequency, radiation wavelength and information transmission distance);
- repeater beam setting accuracy is not worse than 0,05°, which imposes very stringent requirements on the spacecraft position stabilization system;
- implementation of the specified laws of the amplitude-phase distribution over the canvas of the scanning APAA.

At the same time, the APAA of the spacecraft must form a radiation pattern of a special shape that makes it possible to irradiate some areas of the earth's surface without affecting others, as well as provide resistance to the effects of intentional and unintentional interference and the possibility of intercepting radiation.

Known schemes for constructing antenna systems of communication satellites are reflector antennas with a feed in the form of APAA.

2. Formulation of the problem

It is necessary to substantiate the potential technical characteristics of the APAA for different frequency ranges depending on the dimensions of the antenna-feeder system, the spacing between the array elements, etc., to obtain specific values and discuss the results obtained in order to solve the target problem of mobile satellite communications from the spacecraft.

To increase the range and reliability of communication between a ground control station and a satellite device, it is necessary to develop variants of an antenna device with technological simplicity, increased gain and a large field of view in the azimuthal plane. One of the options for solving this problem is the development and use of antennas that provide compactness and simplicity of design, minimization of metallized surfaces, whose electromagnetic parameters are higher or comparable to those of directional multivibrator antennas. The disadvantages of multivibrator antennas of the complex with satellite devices are the mandatory presence of a mechanical drive for the orientation of the antenna device in the azimuthal plane, design complexity, single-beam radiation mode, which can be eliminated by using a beam-forming device such as a Luneberg lens and an antenna array.

The design of a multibeam antenna array proposed in this work will allow: to realize amplification of the emitted signal up to 11-16 *dB*; reduce the metal consumption of the structure, the mass and dimensions of the antenna device; provide a variable sector view in the azimuthal plane up to 360 degrees. The purpose of the work is the development and study of a multi-beam antenna array, in which the dielectric constant is variable and changes according to a certain law.

This antenna array will contain a set of hemispherical axisymmetric dielectric elements of variable thickness and variable diameter, determined in accordance with the change in effective permittivity, and a multi-element phased antenna array of thin-wire vibrators with reflectors structurally placed on a shielded dielectric substrate. In this case, the wall thickness of the dielectric hemispheres decreases stepwise from the center to the periphery, and the air gap between the walls of the hemispheres increases stepwise.

In accordance with this provision, a sample of the antenna array is presented for excitation options with a vibrator as part of the antenna array and one vibrator with a reflector are shown in Figure 1(a) and Figure 1(b), respectively. Based on the developed version of the multi-beam antenna array, a model (Figure 2) was made of polystyrene using 3D printing technology, which has the following characteristics: sticks: weight – 420 *g*, dimensions – 80 × 80 × 50 *mm*.

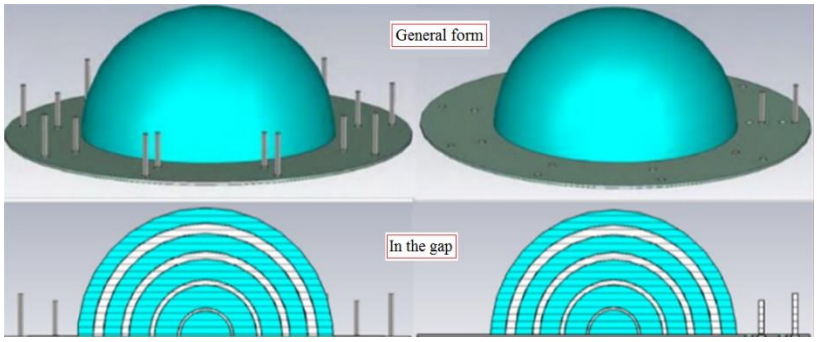

(a) (b)

Figure 1. Antenna options. (a) antenna array sample for excitation options with a vibrator as part of the antenna array. (b) A sample of an antenna array with one vibrator with a reflector

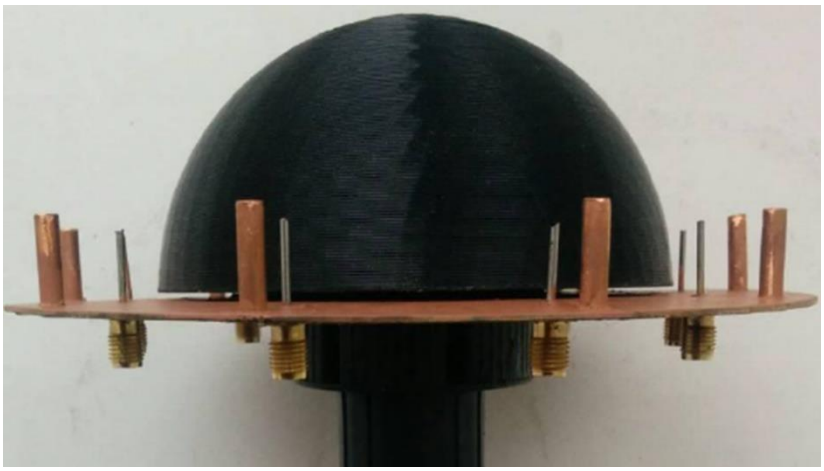

Figure 2. Antenna layout

3. Mathematical apparatus for calculating the main technical characteristics of APAA

APAA are basically described by the same parameters as other classes of antenna systems: the radiation pattern, the width of its main lobe, the level of the side lobes, the gain, the directivity, the reflection coefficients of the elements, and have the same characteristics.

In addition, new energy characteristics are added that reflect the specifics of APAA: potential T and specific noise power spectral density Q.

For the transmitting APAA, the potential is equal to

$$T = G_a T_1 = KU_a P_0 N_e, \tag{1}$$

where G_a is the gain of an APAA (numerically equal to the product of the efficiency factor and the directional factor); P_0 is the radiation power of a single emitter; N_e is the number of single emitters; T_1 is the total potential of all single emitters.

For the receiving APAA, the specific power spectral density of the noise

$$Q = \frac{h_s}{S_{eff}}, \tag{2}$$

where h_s is the noise power spectral density at the APAA output; S_{eff} is the effective surface of the antenna.

The three-dimensional APAA radiation pattern $f(\theta,\varphi)$ in the general case has the form

$$f(\theta,\varphi) = \frac{1}{MN}\left|\frac{\sin\left(M\pi d_x(\sin\theta\cos\varphi)/\lambda\right)}{\sin\left(\pi d_x(\sin\theta\cos\varphi)/\lambda\right)}\right| \times \left|\frac{\sin\left(N\pi d_y(\sin\theta\sin\varphi)/\lambda\right)}{\sin\left(\pi d_y(\sin\theta\sin\varphi)/\lambda\right)}\right|, \tag{3}$$

where M is the number of emitters along the length of the antenna array web; N is the number of emitters along the width of the antenna array web; d_x is the distance between radiators in the azimuthal plane; d_y is the distance between the emitters in the elevation plane; λ is the operating wavelength of the radiation; θ is the azimuth; φ is the elevation angle.

The optimal choice of antenna array dimensions is chosen according to the analytical dependence of the form

$$\begin{cases} d_x \le \dfrac{\lambda}{1+\sin\theta_{\max}^x}, \\ d_y \le \dfrac{\lambda}{1+\sin\theta_{\max}^y}, \end{cases} \tag{4}$$

where $\theta_{\max}^x$, $\theta_{\max}^y$ are the maximum beam opening angles in the azimuth and elevation directions, respectively.

The active APAA module in the time domain can be described by the following system of equations in operator form of the form

$$\begin{cases} U_i = L_i(\vec{e}, i_i), \\ U_o = L_o(i_o), \end{cases} \quad \begin{cases} i_i = F_i(U_i, U_o), \\ i_o = F_o(U_i, U_o), \end{cases} \tag{5}$$

where U_i, U_o, i_i, i_o are the voltages and currents at the input and output of the antenna module, respectively; $\vec{e}$ is a normalized vector; F_i, F_o are generally non-linear integro-differential linearly independent operators describing the active element; L_i, L_o are linear integro-differential operators that describe the input and output circuits of an active element (vacuum lamp, bipolar or field-effect transistor) and are determined by a system of equations of the form

$$\begin{cases} L_i = \sum\limits_{m=0}^{M} a_m^R \dfrac{d^m}{dt^m} + \sum\limits_{n=0}^{N} b_b^R \int\int ... \int dt^n, \\ L_o = \sum\limits_{m=0}^{M} a_m^F \dfrac{d^m}{dt^m} + \sum\limits_{n=0}^{N} b_b^F \int\int ... \int dt^n, \end{cases} \tag{6}$$

where R, F, n, m are the indices of the dimension of the operator space; a, b are weight coefficients.

4. Mathematical modelling basic characteristics of antenna system

Computer simulation was carried out for 16 × 16 *m* APAA at frequencies of 3, 10, 20 and 25 *GHz*. The total number of antenna array elements was 16384 elements (M = 128 elements in the azimuthal plane and N = 128 elements in the elevation plane). The distance between the elements $d_x = d_y$ = 0,1 *m*. On Figure 3(a), (b), (c) shows two-dimensional APAA radiation patterns in the azimuth (elevation) plane at frequencies of 20, 10 and 3 *GHz*, respectively. Due to the symmetry of the design of the active phased antenna array, the radiation patterns in the azimuthal and elevation planes coincide.

Due to the symmetry of the design of the APAA, the radiation patterns in the azimuthal and elevation planes coincide. On Figure 4(a), (b), (c) shows three-dimensional radiation patterns in two parameters (azimuth and elevation) at a frequency of 10 *GHz* APAA sized 128×128, 160×160 and 200×200 elements, respectively (the step between the elements is the same in all cases, equal to 0,125 *m*).

Modeling of the main characteristics of an active phased antenna array makes it possible to determine (analyze) at the design stage the main characteristics of the APAA: the minimum width of the main beam (important in the formation of a multipath radiation pattern), the level of side lobes (characterizes the constructive literacy of the AFAA), the directional properties of the active phased array as a whole.

It is advisable to carry out similar modeling not only in mathematical analysis packages (MathLab, MathCad, Mathematica), but also numerically by writing programs in a high-level language (Borland Delphi, C Sharp, Python). On Figure Figure 5(a), (b), (c), (d) shows the radiation patterns in the azimuth

(elevation) plane, obtained by a numerical method in the Borland Delphi package as superposition of all single emitters for a 128×128 array (0,125 *m* array spacing) at 3, 10, 20, and 25 *GHz*, respectively.

The CST Microwave Studio electrodynamic simulation package allows you to optimize the array according to directivity and efficiency criteria. CST Microwave Studio has an option to set the geometric parameters of the APAA.

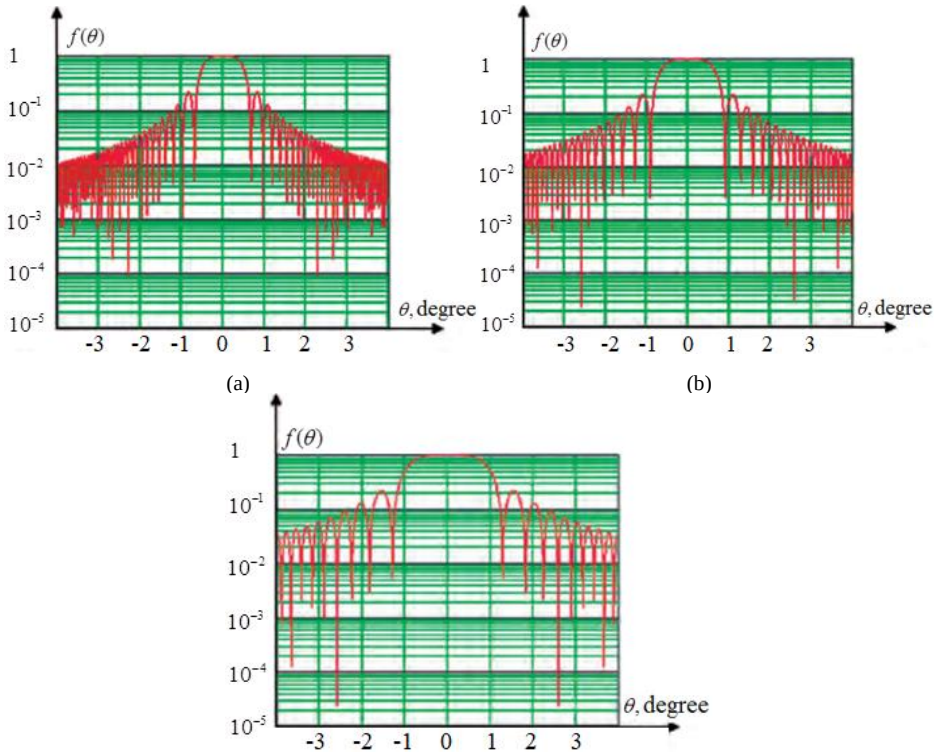

Figure 3. Two-dimensional APAA radiation patterns. (a) For 20 *GHz* frequency. (b) For 10 *GHz* frequency. (c) For 3 *GHz* frequency

On Figure 6 shows the structure of the APAA panel and the initial data for its electrodynamic simulation. On Figure 7(a) and 7(b) show the radiation patterns for a scanning angle of 30° and for a number of scanning angles, respectively. On Figure 8 shows the final three-dimensional APAA radiation pattern at a radiation frequency of 3 *GHz*.

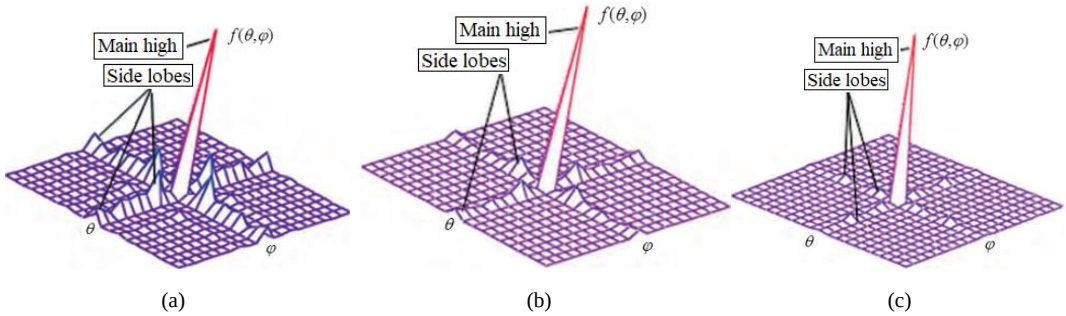

Figure 4. Three-dimensional APAA radiation patterns. (a) For APAA sized 128×128. (b) For APAA sized 160×160. (c) For APAA sized 200×200

It should be noted that computer modeling makes it possible already at the stage of the draft design to quantify the main technical characteristics of an active phased antenna array: the width of the central beam of the radiation pattern, the gain, the level of the side lobes, the directivity. Based on these characteristics, it is possible to present specific requirements for the geometric parameters of the APAA, the number and power of single emitters, the length and width of the array, and the step between the emitters.

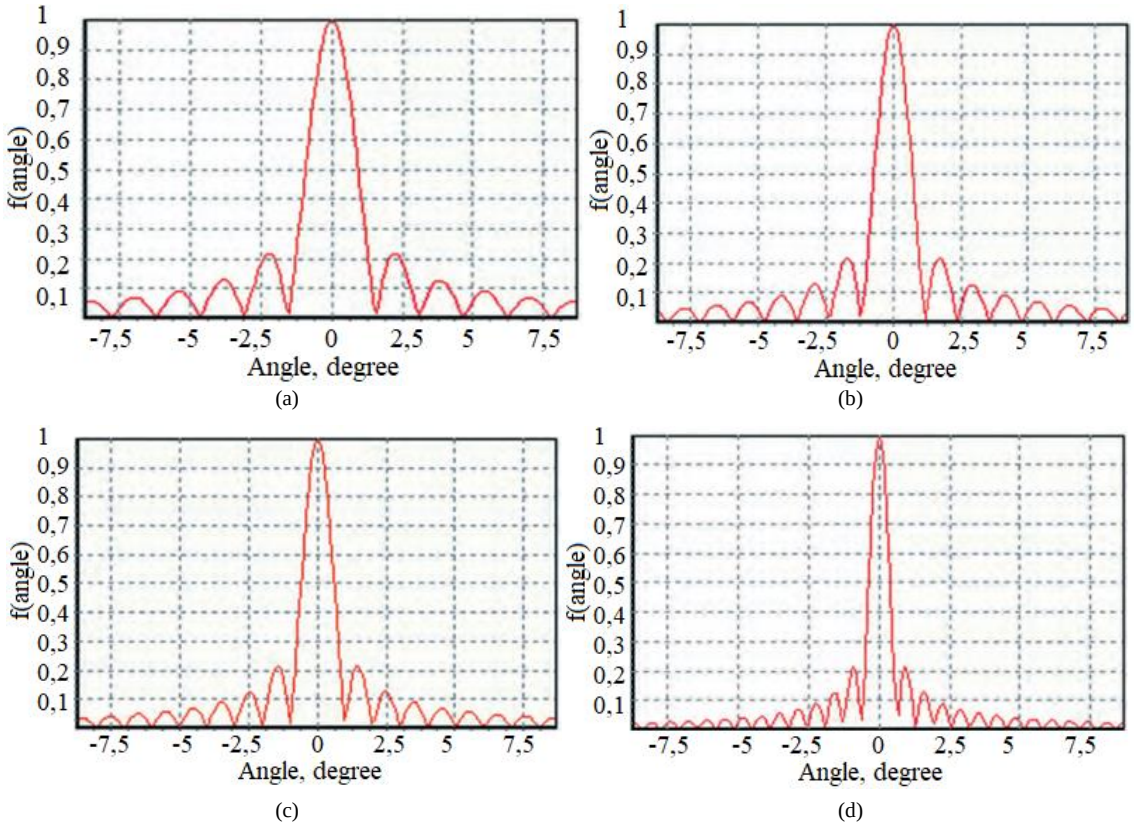

Figure 5. Directional patterns of symmetrical APAA, obtained by numerical method. (a) For 3 *GHz* frequency. (b) For 10 *GHz* frequency. (c) For 20 *GHz* frequency. (d) For 25 *GHz* frequency

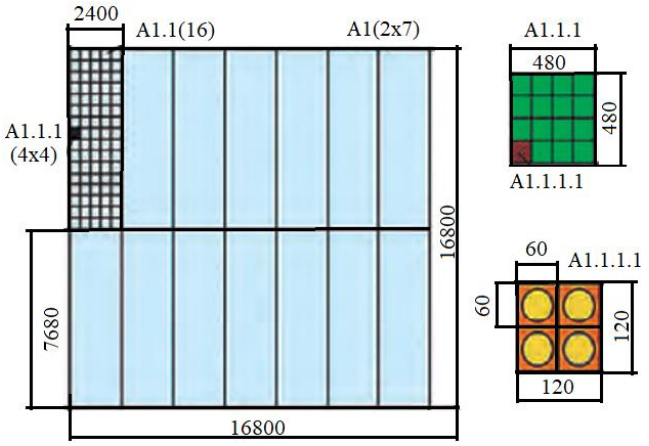

Figure 6. Structure of the APAA panel

5. Results and discussion

Computer modeling and analytical calculations have shown that with an equivalent isotropically radiated power of 85 *dBWt* from the spacecraft, the target communication problem is guaranteed to be solved, in this case, the power flux density at the input of the satellite earth station will be at least minus 84 *dBWt* in the signal band (diagram width directivity of the APAA in this case will be no more than 0,7 × 0,7°).

With an increase in the width of the APAA radiation pattern to 1×1°, the power flux-density will be minus 90 *dBWt*, at 1,5×1,5° - minus 98 *dBWt*, at 2,5×2,5°- minus 110 *dBWt*, at 5×5° - minus 125 *dBWt*, at 7×7° - minus 138 *dBWt*. As practice shows (Abdulrahman *et al.*, 2021), at the input of the earth station of a satellite communication system, a power flux-density level of at least 158 *dBWt* is required (Figure 7).

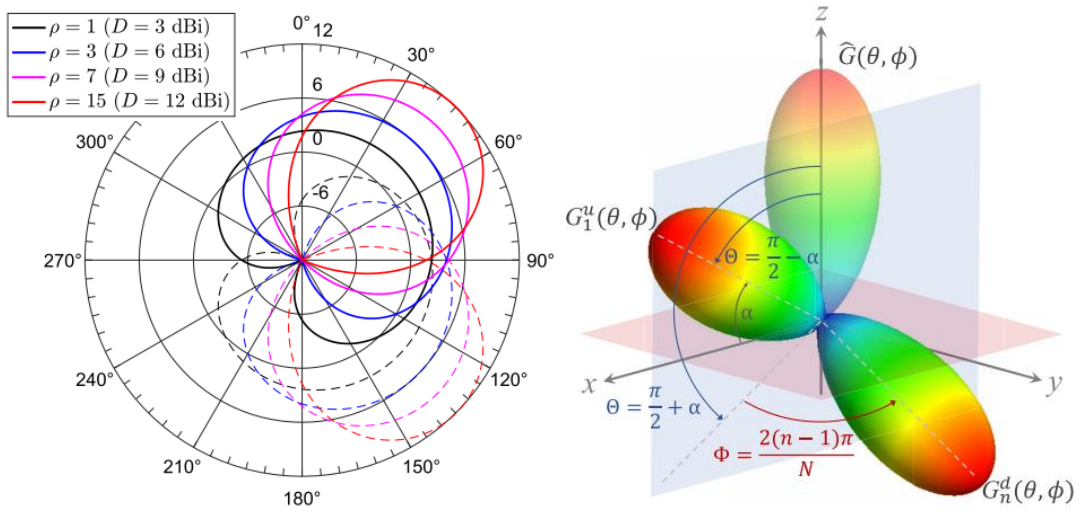

(a) (b)

Figure 7. Modeling of APAA in the polar coordinate system. (a) Ordinary radiation patterns. (b) 3D radiation patterns

Thus, APAA with a transmitter of 85 *dBWt* is guaranteed to solve the target problem of providing mobile satellite communications with both one global beam and a plurality of beams with a width of 0,7 × 0,7°. It should be added that the advantage of forming multiple beams compared to a global beam with one APAA is: a higher data rate, relatively low requirements for antenna systems of ground stations, greater noise immunity of the radio link, the ability to dynamically control the signal power in each beam (Figure 8).

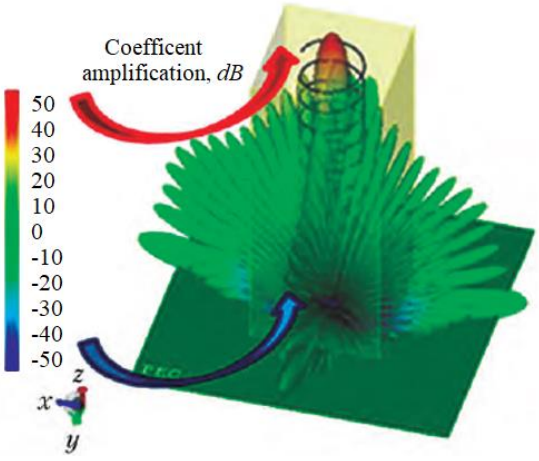

Figure 8. Electrodynamic modeling of APAA

From the energy standpoint, the APAA with a size of 16 × 16 *m* helps to ensure a gain of 50 *dB* and the formation of a minimum width of the central beam of the directional pattern of 0,45 × 0,45°, which makes it possible to form a local beam with a diameter of 230 *km* on the Earth's surface.

Three-dimensional active phased array radiation patterns allow one to quantify the levels of side lobes in the azimuth and elevation planes depending on the operating frequency, the spacing between the array elements and the number of elements in the array.

For the numerical analysis of the synthesized structure, the finite integration method was used. The numerical experiment was carried out using the CST Studio Suite software and methodological complex with the developed antenna structure in various combinations and made it possible to form groups of electrodynamic characteristics to assess the possibility of using this antenna as part of the equipment of ground control stations of radio engineering complexes.

At the first stage of the experiment, the mode of operation of the model with one asymmetric half-wave vibrator, which excited the antenna structure, was studied. The calculated radiation patterns are shown in Figure 9. The primary analysis of the radiation patterns initiated the introduction of a structural element of the reflector to reduce the level of the rear radiation lobe.

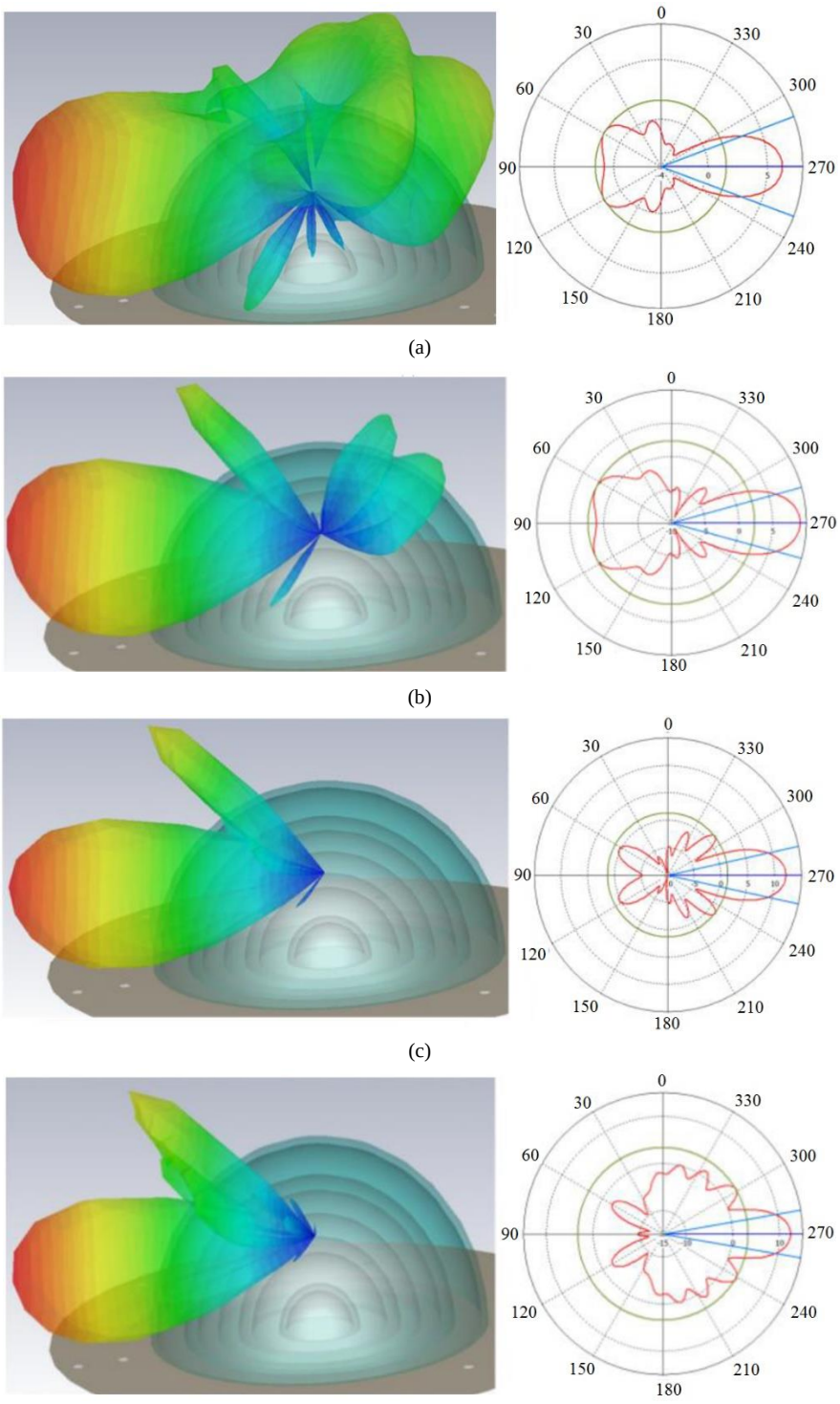

Figure 9. Antenna patterns with one vibrator: (a) frequency 4 *GHz*, gain 6,26 *dB*, main lobe width 41,1 degrees; (b) frequency 5,6 *GHz*, gain 9,06 *dB*, width of the main petal 30,9 degrees; (c) frequency 6 *GHz*, gain 12,1 *dB*, main lobe width 24,4 degrees; (d) frequency 7 *GHz*, gain 12,4 *dB*, main lobe width 19,5 degrees

A sample of a multi-beam antenna array is supposed to be used in multi-beam reception-transmission modes or single-beam electron scanning in a wide azimuth sector. A numerical experiment of this antenna structure as part of a hemispherical lens and an antenna array made it possible to obtain the characteristics shown in Figure 10. An increase in the number of antenna elements led to the expected expansion of the main radiation lobe and a decrease in the gain, as well as an increase in the level of the back and side lobes. As the frequency of the signal increases, the radiation pattern begins to “fall apart”, but the gain decreases slightly.

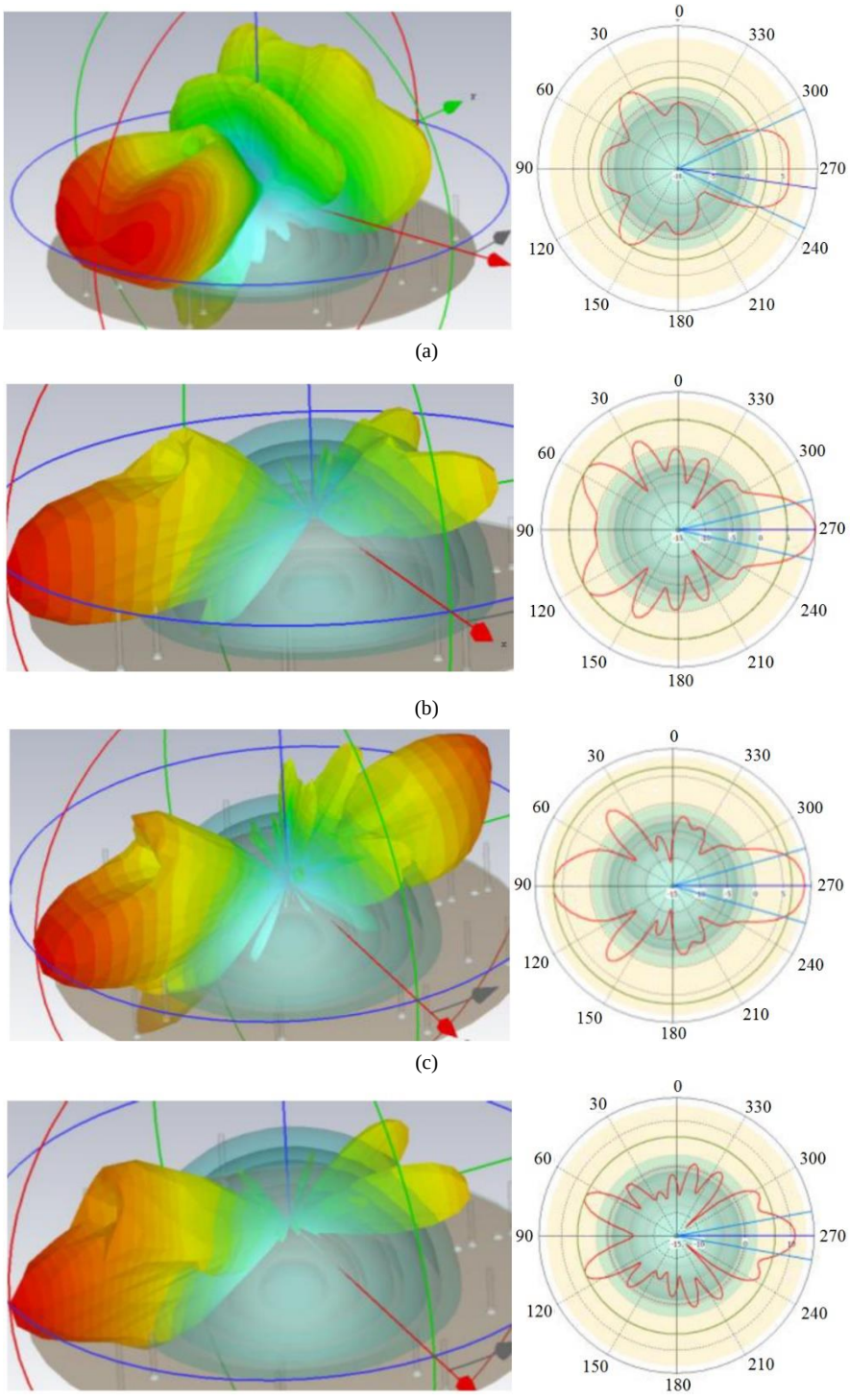

Figure 10. Directional patterns for an antenna system containing a phased antenna array: (a) frequency 4 *GHz*, gain 5,97 *dB*, main lobe width 49,4 degrees; (b) frequency 5,6 *GHz*, gain 9,87 *dB*, width of the main petal 25,4 degrees; (c) frequency 6 *GHz*, gain 8,83 *dB*, main lobe width 31,9 degrees; (d) frequency 7 *GHz*, gain 10,9 *dB*, main lobe width 20,3 degrees

In order to improve the characteristics of a multibeam antenna array (directivity, matching with the feeder path, expanding the frequency range), more complex elements, such as patch antennas, Vivaldi antennas, horn antennas, can be used as active components of the antenna array.

The ongoing research on changing the geometric dimensions of the lens structure revealed a pattern - an increase in the radius of a hemispherical lens numerically up to 5 lengths waves leads to a decrease in the width of the main lobe of the radiation pattern by almost an order of magnitude and an increase in the gain, as shown in Figure 11.

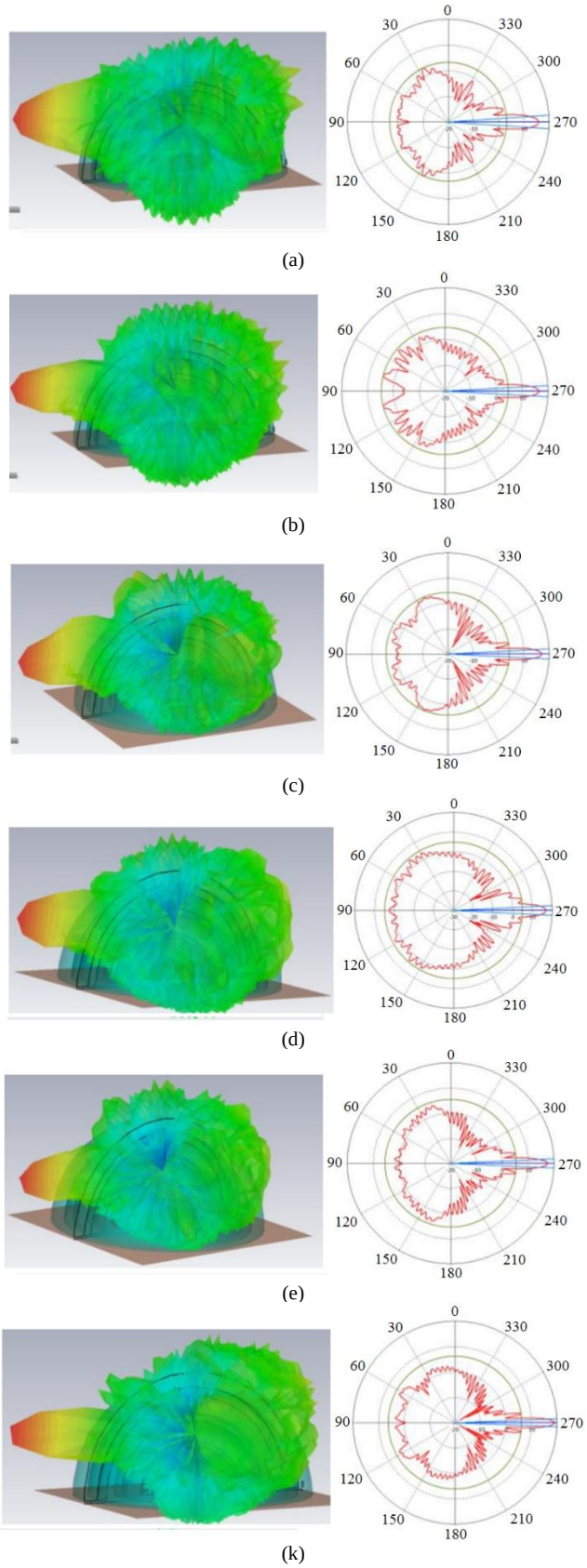

Figure 11. Antenna patterns with an increased radius of the Luneberg lens: (a) frequency 4 *GHz*, gain 15,7 *dB*, main lobe width 7,4 degrees; (b) frequency 4,8 *GHz*, gain 16,5 *dB*, width of the main petal 6,2 degrees; (c) frequency 5 *GHz*, gain 16,9 *dB*, main lobe width 6 degrees; (d) frequency 5,6 *GHz*, gain 16,7 *dB*, main lobe width 5,7 degrees; (e) frequency 6 *GHz*, gain 17,4 *dB*, main lobe width 5,2 degrees; (k) frequency 7 *GHz*, gain 19,6 *dB*, main lobe width 4,6 degrees

6. Conclusions

The results obtained allow us to formulate a number of provisions on the quality indicators of the antenna device:

1. A multi-beam antenna array based on a hemispherical dielectric multilayer lens provides a gain in the range of 5-12 *dB*, which is comparable to the gain of known directional multivibrator antennas.
2. Due to the selection of radiating antenna elements, which can be Vivaldi antennas, horn antennas, patch antennas and other types of directional and non-directional antenna elements, it is possible to change the energy level, set the frequency range and the mode of matching with the antenna-feeder path.
3. It is possible to realize multipath or scanning mode of operation.
4. A multi-beam antenna array based on a hemispherical dielectric multilayer lens has smaller weight and size indicators, as well as metal consumption compared to antennas of a similar purpose.
5. It is possible to install a multi-beam antenna array based on a hemispherical dielectric multilayer lens on mobile carriers under a radio-transparent dome.

Acknowledgements

The authors would like to thank the editor and anonymous reviewers for constructive, valuable suggestions and comments on the work.

References

1. Abdulrahman, S. M. A., Anthony, E. S., Konstanty, S. B., and Amin A. (2021) Flexible meander-line antenna array for wearable electromagnetic head imaging. *IEEE Transactions on Antennas and Propagation*, 69(7), 4206-4211.
2. Ao, L., and KwaI-Man, L. (2020) Single-layer wideband end-fire dual-polarized antenna array for device-to-device communication in 5G wireless systems. *IEEE Transactions on Vehicular Technology*, 69(5), 5142-5150.
3. Avishek, D., Durbadal, M., and Rajib, K. (2021) An optimal circular antenna array design considering the mutual coupling employing ant lion optimization. *International Journal of Microwave and Wireless Technologies*, 13(2), 164-172.
4. Botao, F., Liangying, L., Kwok, L. C., and Yansheng, L. (2020) Wideband widebeam dual circularly polarized magnetoelectric dipole antenna/array with meta-columns loading for 5G and beyond. *IEEE Transactions on Antennas and Propagation*, 69(1), 219-228.
5. Daniel, C., Stavros, V., and Jeffrey, A. N. (2022) Imageless shape detection using a millimeter-wave dynamic antenna array and noise illumination. *IEEE Transactions on Microwave Theory and Techniques*, 70(1), 758-765.
6. Islamov, I. J., and Ismibayli, E. G. (2018) Experimental Study of Characteristics of Microwave Devices Transition from Rectangular Waveguide to the Megaphone. *IFAC-PapersOnLine*, 51(30), 477-479.
7. Islamov, I. J., Hasanov, M. H., and Abbasov, M. H. (2021) Simulation of Electrodynamic Processes in a Cylindrical-Rectangular Microwave Waveguide Systems Transmitting Information. *11th International Conference on Theory and Application of Soft Computing, Computing with Words, Perception and Artificial Intelligence*, 4, 246-253.
8. Islamov, I. J., Hunbataliyev, E. Z., Abdullayev, R. Sh., Shukurov, N. M., and Hashimov, Kh. Kh. (2021) Modelling of a Microwave Rectangular Waveguide with a Dielectric Layer and Longitudinal Slots. *International Symposium for Production Research*, 6, 550-558.
9. Islamov, I. J., Hunbataliyev, E. Z., and Zulfugarli, A. E. (2021) Numerical Simulation of Characteristics of Propagation of Symmetric Waves in Microwave Circular Shielded Waveguide with a Radially Inhomogeneous Dielectric Filling. *International Journal of Microwave and Wireless Technologies*, 9, 761-767.
10. Islamov, I. J., Ismibayli, E. G., Gaziyev, Y. G., Ahmadova, S. R., and Abdullayev, R. Sh. (2019) Modeling of the Electromagnetic Feld of a Rectangular Waveguide with Side Holes. *Progress in Electromagnetics Research*, 81, 127-132.
11. Islamov, I. J., Ismibayli, E. G., Hasanov, M. H., Gaziyev, Y. G., and Abdullayev, R Sh. (2018) Electrodynamics Characteristics of the No Resonant System of Transverse Slits Located in the Wide Wall of a Rectangular Waveguide. *Progress in Electromagnetics Research Letters*, 80, 23-29.

12. Islamov, I. J., Ismibayli, E. G., Hasanov, M. H., Gaziyev, Y. G., Ahmadova, S. R., and Abdullayev, R. Sh. (2019) Calculation of the Electromagnetic Field of a Rectangular Waveguide with Chiral Medium. *Progress in Electromagnetics Research*, 84, 97-114.
13. Islamov, I. J., Shukurov, N. M., Abdullayev, R. Sh., Hashimov, Kh. Kh., and Khalilov, A. I. (2020) Diffraction of Electromagnetic Waves of Rectangular Waveguides with a Longitudinal. *Wave Electronics and its Application in Information and Telecommunication Systems*, 19806145, 35-46.
14. Ismibayli, E. G., and Islamov, I. J. (2018) New Approach to Definition of Potential of the Electric Field Created by Set Distribution in Space of Electric Charges. *IFAC-PapersOnLine*, 51(30), 410-414.
15. Kai, G., Xiaoxiang, D., Li, G., Yanwen, Z., and Zaiping, N. (2021) A broadband dual circularly polarized shared-aperture antenna array using characteristic mode analysis for 5G applications. *International Journal of RF and Microwave Computer-Aided Engineering*, 31(3), 234-243.
16. Khalilov, A. I, Islamov, I. J., Hunbataliyev, E. Z., Shukurov, N. M., and Abdullayev, R. Sh. (2020) Modeling Microwave Signals Transmitted Through a Rectangular Waveguide. *Wave Electronics and its Application in Information and Telecommunication Systems*, 19806152, 56-67.
17. Mohammad, M. F. (2020) A wideband rectenna using high gain fractal planar monopole antenna array for RF energy scavenging. *International Journal of Antennas and Propagation*, 3489323, 1-10.
18. Muhammad, M. H., Muzhair, H., Adnan, A. K., Imran, R., and Farooq, A. B. (2021) Dual-band B-shaped antenna array for satellite applications. *International Journal of Microwave and Wireless Technologies*, 3(8), 851-858.
19. Pinuela, M., Mitcheson, P. D., and Lucyszyn, S. (2013) Ambient RF energy harvesting in urban and semi-urban environments. *IEEE Transactions on Microwave Theory and Techniques*, 61(7), 2715-2726.
20. Yi-Ming, Z., Shuai, Z., Guangwei, Y., and Gert, F. P. (2020) A wideband filtering antenna array with harmonic suppression. *IEEE Transactions on Microwave Theory and Techniques*, 68(10), 4327-4339.
21. Yuchen, M., Junhong, W., Zheng, L., Yujian, L., Meie, C., and Zhan, Z. (2020) Planar annular leaky-wave antenna array with conical beam. *IEEE Transactions on Antennas and Propagation*, 68(7), 5405-5414.
22. Zhao, Y., Guangjun, W., Wei, H., Daniele, I., Yongjun, H., and Jian, L. (2020) Microwave airy beam generation with microstrip patch antenna array. *IEEE Transactions on Antennas and Propagation*, 69(4), 2290-2301.
23. Zhou, M., Shojaei BaghinI, M., and Kumar, G. (2016) Broadband bent triangular omnidirectional antenna for RF energy harvesting. *IEEE Antennas and Wireless Propagation Letters*, 15, 36-39.